

# Femtosecond laser fabricated micro Mach-Zehnder interferometer with Pd film as sensing materials for hydrogen sensing

Min Wang,<sup>1,\*</sup> Minghong Yang,<sup>1</sup> Jie Cheng,<sup>1</sup> Jixiang Dai,<sup>1</sup> Minwei Yang,<sup>2</sup> and D. N. Wang<sup>2</sup>

<sup>1</sup>National Engineering Laboratory for Fiber Optic Sensing Technology, Wuhan University of Technology, 122 Luoshi Road, Wuhan, China, 430070

<sup>2</sup>Department of Electrical Engineering, The Hong Kong Polytechnic University, Hong Kong, China

\*Corresponding author: bluebluecherry@163.com

Received January 17, 2012; revised March 8, 2012; accepted April 6, 2012;  
posted April 9, 2012 (Doc. ID 161495); published May 25, 2012

In this paper, a femtosecond laser fabricated fiber inline micro Mach-Zehnder interferometer with deposited palladium film for hydrogen sensing is presented. Simulation results show that the transmission spectrum of the interferometer is critically dependent on the microcavity length and the refractive index of Pd film and a short microcavity length corresponds to a high sensitivity. The experimental results obtained in the wavelength region of 1200–1400 nm, and in the hydrogen concentration range of 0–16%, agree well with that of the simulations. The developed system has high potential in hydrogen sensing with high sensitivity. © 2012 Optical Society of America  
OCIS codes: 060.2370, 310.6860, 320.2250, 320.7140.

In recent years, optical fiber sensor has attracted more and more attention in academic and industrial communities. The advantages provided by the optical fiber sensor include small size, light weight, high sensitivity and immunity to electromagnetic interference, which facilitate the measurement of a variety of physical, chemical, and biomedical parameters [1–3].

Femtosecond (fs) laser processing is an emerging field with important application prospects. Fs laser has been widely used for micromachining because of its good beam quality, high precision and excellent spatial resolution, which are particularly suitable for fabricating microcavity in the optical fiber. Various structures of microinterferometer cavity have been created by fs laser and used as optical fiber sensors [4–8]. Especially, an ultracompact microcavity Mach-Zehnder interferometer (MMZI) fabricated by fs laser has been used for measuring refractive index (RI) and different mixture ratios of N<sub>2</sub> and He gases [6,9]. MMZI has also been proposed for temperature measurement and the sensitivity achieved is ~0.046 nm/°C within the temperature ranging from 100 °C to 1100 °C [10–16].

In this paper, an fs laser-fabricated MMZI fiber hydrogen sensor is proposed and developed. A palladium (Pd) film is deposited on the MMZI by magnetron sputtering process to be used as the transducer layer between the gas and the optical fiber waveguide for monitoring hydrogen concentrations. The MMZI coated with the Pd film is analyzed and discussed under different conditions such as different microcavity lengths and different hydrogen concentrations. The experimental results obtained show that transmission spectrum of the MMZI varies with the the hydrogen concentration and the period of the spectrum is dependent on the microcavity length, which agrees with the simulated results.

In principle, there are two main light transmission paths on the MMZI coated with the Pd film according to the traditional theory of MMZI. Figure 1 shows the schematic structure and digital microscope (VHX-100) images of the MMZI which are fabricated by fs laser ablation.

The interference intensity can be expressed by [17]

$$I = I_1 + I_2 + 2\sqrt{I_1 I_2} \cos \varphi, \quad (1)$$

where  $I_1$  and  $I_2$  are the intensities along the two light paths and  $\varphi$  is the phase difference to be defined as

$$\varphi = 2\pi\Delta n_{\text{eff}}L/\lambda + \varphi_0, \quad (2)$$

where  $\Delta n_{\text{eff}}$  is the RI difference between the fiber core and the microcavity;  $\lambda$  is the wavelength;  $L$  is the length of the microcavity, and  $\varphi_0$  is the initial interference phase.

$$\Delta n_{\text{eff}}L = 2(n_{\text{film}} - n_{\text{core}})d_{\text{film}} + (n_{\text{cavity}} - n_{\text{core}})(L - 2d_{\text{film}}), \quad (3)$$

where  $n_{\text{film}}$  is the RI of the Pd film;  $n_{\text{core}}$  is the RI of the fiber core;  $n_{\text{cavity}}$  is the RI of the micro-cavity and  $d_{\text{film}}$  is the thickness of the Pd film.

The RI values of the fiber core  $n_{\text{core}}$  and the microcavity  $n_{\text{cavity}}$  are 1.4682 and 1.000132 respectively [9]. Wavelength  $\lambda$  used in the simulations is between 1200 and 1400 nm. The microcavity lengths  $L$  adopted are 40 and 100  $\mu\text{m}$  respectively, and the  $n_{\text{film}}$  values ranging from 2.7 to 3 are used in the simulation. The imagery part of the Pd refractive index can influence the intensity of light which has almost no effect on phase variation. Thus, it can be ignored in the formula of phase shift calculation. The simulated results using Rsoft optical design software (RSoft, Inc.) show that the change of effective RI of the light propagating inside the core can be five orders of magnitude smaller than that of the complex RI of the coated Pd film, and hence can be neglected.

As shown in Fig. 2(a), the simulated results show that the spectral period change is mainly determined by the microcavity lengths and a shorter microcavity corresponds to a larger spectral period. Taking the microcavity length of 40  $\mu\text{m}$ , a red shift of wavelength appears

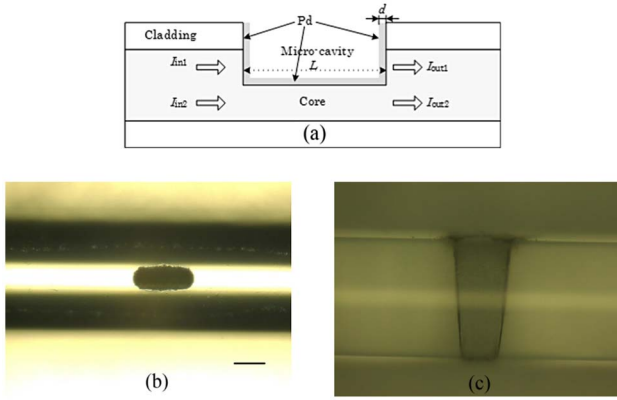


Fig. 1. (Color online) Schematic structure and digital microscope images of MMZI fabricated by fs laser ablation with a  $50\ \mu\text{m}$  scale bar. (a) Structural illustration; (b) top view; (c) side view.

when the RI of the Pd film changes from 3 to 2.7 in Fig. 2(b). The experimental results show that a small microcavity length corresponds to a large wavelength shift, which agrees well with the simulated results. From Fig. 2(c), the slopes of wavelength shift at a specific RI of the coated Pd film with certain thickness calculated at different microcavity lengths of 20, 40, and  $100\ \mu\text{m}$ , respectively. In the simulation, the slopes corresponding to the microcavity lengths of 20, 40, and  $100\ \mu\text{m}$  are 0.0296, 0.0145, and  $0.0057\ \text{nm}/\text{RIU}$ , respectively. It can be concluded that a small microcavity length corresponds to a large wavelength shift.

A single-mode fiber (SMF) with core and cladding diameters of  $8.2$  and  $125\ \mu\text{m}$  is used in the experiments. The fs laser system is divided into four subsystems, including the fs laser (Spectral Physics), optical system, CCD monitoring system, and three-dimensional moving working platform. The fs laser has been utilized to fabricate the MMZI, where the specific parameters are as follows: central wavelength of  $800\ \text{nm}$ , pulse width of  $120\ \text{fs}$ ,

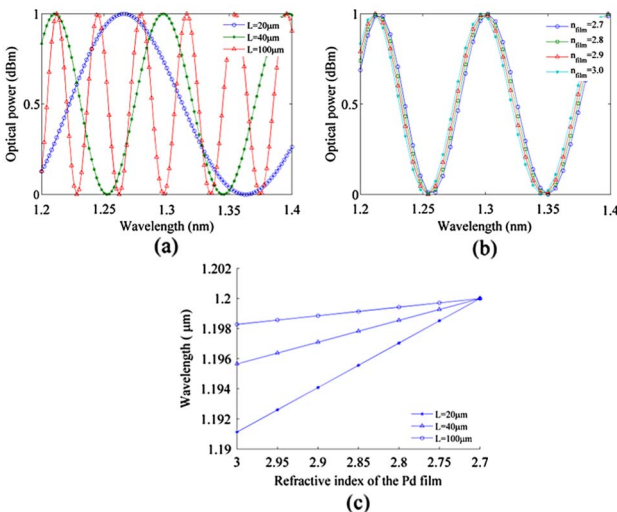


Fig. 2. (Color online) (a) transmission spectra of MMZI with different microcavity lengths; (b) transmission spectra of MMZI coated with Pd film between 3 and 2.7,  $L = 40\ \mu\text{m}$ ,  $d_{\text{film}} = 110\ \text{nm}$ ; (c) wavelength versus the refractive index of the coated Pd film.

repetition rate of  $1\ \text{kHz}$ , and the average on-target laser power was maintained at  $12\ \text{mW}$ . Ultra high vacuum (UHV) magnetron sputter system from BESTEC Germany is used to deposit the Pd films on the MMZI over SMF by direct current sputtering. The influence of hydrogen to different MMZI coated with the Pd film in various hydrogen concentration conditions is tested. The wavelength shifts of transmission spectra are recorded by Optical Spectrum Analyzer (AQ6370B). In the experiments, the microcavity lengths are 40 and  $100\ \mu\text{m}$  respectively, measured using digital microscope imaging. The thickness of the Pd film is  $\sim 110\ \text{nm}$ , calculated by the deposition velocity and time. Meanwhile, Pd film is deposited on an Si substrate to be used as the standard reference to measure film thickness and to improve measurement precision. Various RI values of the Pd films are provided by changing the flowing rate of  $\text{H}_2$  gases.

Figure 3 illustrates the shifts of the wavelength coated with  $110\ \text{nm}$  Pd film under different hydrogen concentrations. By comparing Figs. 3(a) and 3(c), it can be found that the period of spectrum with microcavity length of  $40\ \mu\text{m}$  is larger than that of the microcavity length of  $100\ \mu\text{m}$ . The experimental results agree with the simulated results shown in Fig. 2(a).

It can also be observed from Figs. 3(b) and 3(d) that MMZI spectra experience a red shift. According to the former report, the Pd film changes its complex RI with the variation of hydrogen concentration [18]. The wavelength shift of the transmission spectra is induced by the expansion of Pd film, following the increase of the hydrogen volume ratio from 0 to 16%. Finally, when air is filled into the chamber again, the transmission spectrum will return to its original location after ten minutes and the experimental results are repeatable.

In the simulation, it can be found that at a certain thickness of the Pd film, the shift of the wavelength becomes larger when the microcavity length is shorter, as demonstrated in Fig. 2(c). In the experiment, the Pd film expands with the increase of hydrogen concentration, which is caused by the decreased complex RI of Pd with

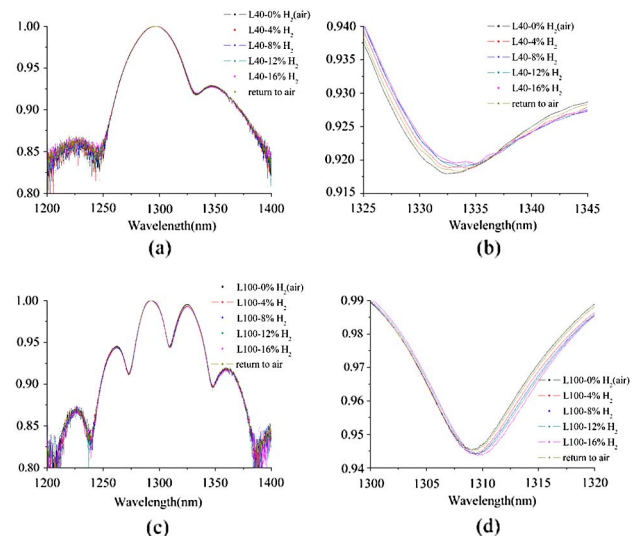


Fig. 3. (Color online) Normalized transmission spectra of MMZI coated with Pd film of  $110\ \text{nm}$  in thickness (a)–(b)  $L = 40\ \mu\text{m}$ ; (c)–(d)  $L = 100\ \mu\text{m}$ .

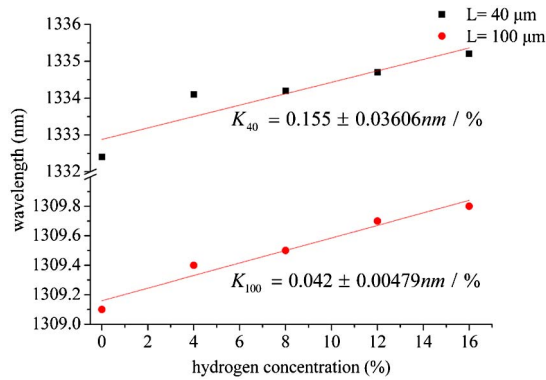


Fig. 4. (Color online) Wavelength versus hydrogen concentration in different micro-cavity lengths of  $L = 40 \mu\text{m}$  and  $L = 100 \mu\text{m}$ .

the increased absorption of hydrogen. The wavelength shift increases because of the reduction of the microcavity length, as the Pd film expands and its RI is decreased with the increase of the hydrogen in 0 to 16% volume concentration.

Figure 4 shows the relationship between the wavelength shift and the hydrogen concentration. The parameter  $K$ , i.e., the slope which is obtained from the linear fitting of the relationship between the hydrogen concentration and the wavelength shift, is introduced to evaluate the sensitivity of the MMZI. The slope for the  $40 \mu\text{m}$  microcavity length is  $\sim 0.155 \text{ nm}/\%$ , which is larger than that of the  $100 \mu\text{m}$  microcavity ( $\sim 0.042 \text{ nm}/\%$ ). This means that the MMZI with  $40 \mu\text{m}$  microcavity length has larger wavelength shift than that of the  $100 \mu\text{m}$  microcavity.

It should be mentioned that the side surface made by fs laser could not be smooth but coarse and irregular, and that it is not easy to remove the particles as small as  $1 \mu\text{m}$  in diameter. Furthermore, the temperature and humidity also affect the performance of the MMZI coated with Pd film. For the sake of simplicity, the influence of the RI variation of hydrogen-air mixture on transmission spectra is not accounted for in this paper. However, the experimental results obtained still agree well with that of the simulations, which reveal the potential of the MMZI coated with Pd film for hydrogen concentration detection.

In conclusion, the MMZI coated with Pd film as a hydrogen sensing element has been proposed and developed. The transmission spectrum of the sensor system depends on the microcavity length and the wavelength shift is induced by the RI change of the Pd film coated. The system developed has high potential for hydrogen concentration detection.

This work is finally supported by the Project of National Natural Science Foundation of China (NSFC) (Grant No. 60908020), State Education Ministry, and Program for New Century Excellent Talents in University (NCET-10-0664).

## References

1. T. W. Kao and H. F. Tayler, *Opt. Lett.* **21**, 615 (1996).
2. Y. J. Rao, *Opt. Fiber Technol.* **12**, 227 (2006).
3. Y. J. Rao, Y. P. Wang, Z. L. Ran, and T. Zhu, *J. Lightw. Technol.* **21**, 1320 (2003).
4. Y. J. Rao, M. Deng, D. W. Duan, X. C. Yang, T. Zhu, and G. H. Cheng, *Opt. Express* **15**, 14123 (2007).
5. T. Wei, Y. Han, H. L. Tsai, and H. Xiao, *Opt. Lett.* **33**, 536 (2008).
6. Y. Wang, M. W. Yang, D. N. Wang, S. Liu, and P. Lu, *J. Opt. Soc. Am. B* **27**, 370 (2010).
7. Y. Wang, D. N. Wang, M. W. Yang, W. Hong, and P. X. Lu, *Opt. Lett.* **34**, 3328 (2009).
8. C. H. Lin, L. Jiang, H. Xiao, Y. H. Chai, S. J. Chen, and H. L. Tsai, *Opt. Lett.* **34**, 2408 (2009).
9. L. Jiang, L. Zhao, S. Wang, J. Yang, and H. Xiao, *Opt. Express* **19**, 17591 (2011).
10. S. W. James and R. P. Tatam, *Meas. Sci. Technol.* **14**, R49 (2003).
11. J. H. Lim, H. S. Jang, K. S. Lee, J. C. Kim, and B. H. Lee, *Opt. Lett.* **29**, 346 (2004).
12. D. Monzón-Hernández, V. P. Minkovich, and J. Villatoro, *IEEE Photon. Technol. Lett.* **18**, 511 (2006).
13. P. Lu, L. Men, K. Sooley, and Q. Chena, *Appl. Phys. Lett.* **94**, 131110 (2009).
14. J. Villatoro and D. Monzón-Hernández, *J. Lightw. Technol.* **24**, 1409 (2006).
15. H. Y. Choi, M. J. Kim, and B. H. Lee, *Opt. Express* **15**, 5711 (2007).
16. Y. Wang, Y. Li, C. Liao, D. N. Wang, M. Yang, and P. Lu, *IEEE Photon. Technol. Lett.* **22**, 39 (2010).
17. Y. Jung, S. Lee, B. H. Lee, and K. Oh, *Opt. Lett.* **33**, 2934 (2008).
18. K. Schroeder, W. Ecke, and R. Willsch, *Opt. Lasers Eng.* **47**, 1018 (2009).